PHYSICAL REVIEW A **112**, 042409 (2025)

Scalable and fault-tolerant preparation of encoded k-uniform states

Shayan Majidy,[1,*] Dominik Hangleiter,[2] and Michael J. Gullans[3]
[1]*Department of Physics, Harvard University, Cambridge, Massachusetts 02138, USA*
[2]*Simons Institute for the Theory of Computing, University of California, Berkeley, Berkeley, California 94720, USA*
[3]*Joint Center for Quantum Information and Computer Science, University of Maryland and NIST, College Park, Maryland 20742, USA*

(Received 24 March 2025; accepted 17 September 2025; published 3 October 2025)

k-uniform states are valuable resources in quantum information, enabling tasks such as teleportation, error correction, and accelerated quantum simulations. However, the practical realization of k-uniform states, at scale, faces major obstacles: Verifying k uniformity is as difficult as measuring code distances, and devising fault-tolerant logical preparation protocols further adds to the complexity. To address these challenges, we present a scalable fault-tolerant method for preparing encoded k-uniform states and we illustrate our approach using surface and color codes. We first present a technique to determine k uniformity of stabilizer states directly from their stabilizer tableau. We then identify a family of Clifford circuits that ensures both fault tolerance and scalability in preparing these states. Building on the encoded k-uniform states, we introduce a hybrid physical-logical strategy that retains some of the error-protection benefits of logical qubits while lowering the overhead for implementing arbitrary gates compared to fully logical algorithms. We show that this hybrid approach can outperform fully physical implementations for resource-state preparation, as demonstrated by explicit constructions of k-uniform states.

DOI: 10.1103/cl23-c3jg

I. INTRODUCTION

A pure N-qubit state is called k uniform if every subset of k qubits is maximally mixed [1–3]. Such states are used in many quantum information processing tasks, including conventional and open-destination quantum teleportation [4,5], secret sharing [4,5], information masking [6], benchmarking [7], and quantum error correction [8–14]. Well-known examples include the Greenberger-Horne-Zeilinger (GHZ) state ($k = 1$), the five-qubit code ($k = 2$) [15], and the toric code ($k = 3$) [16]. More generally, any logical state of a stabilizer code with pure distance d_p (minimum weight undetectable error [17]) is a $(d_p - 1)$-uniform state. Beyond these direct applications, k-uniform states also appear in the black-hole–qubit correspondence [18–20], underlie states that can be employed as quantum repeaters [21], and provide extreme realizations of local thermalization [22], thereby further bridging thermodynamics and error correction [23,24]. They have also recently been shown to accelerate quantum simulations [25].

Given their wide-ranging applications, considerable effort has been devoted to identifying k-uniform states. Techniques include brute-force numerical searches [26], graph-state constructions [27–32], combinatorial design methods [33–39], and tools from statistical mechanics [40,41]. In the same vein, there have been parallel efforts to construct proofs of both the existence and the nonexistence of k-uniform states [42–48].

Despite these constructive advances, the practical realization of k-uniform states at scale remains challenging. The first major obstacle is verification as N increases: Confirming k uniformity requires measuring the reduced density matrices of all $\binom{N}{k}$ subsets, a task equivalent to determining the distance of a quantum code, an NP-hard problem. The second, and more fundamental, challenge is fault-tolerant state preparation. Any practical application of k-uniform states must contend with noise and scalability, necessitating logical encoding and fault-tolerant methods for state preparation. Yet, no general framework exists for preparing encoded k-uniform states in a fault-tolerant manner. With quantum computing entering an era where logical qubits and fault-tolerant protocols are becoming experimentally viable [49–59], addressing these challenges is now timely.

In this work we present a numerical method to identify k-uniform stabilizer states which can be prepared fault tolerantly in a natural way. No known application depends on whether a k-uniform state is a stabilizer or nonstabilizer state. Therefore, focusing on stabilizer k-uniform states does not restrict the generality of our analysis. Our approach leverages the stabilizer-tableau formalism to verify k uniformity and systematically searches for families of Clifford circuits that are constant depth, fault tolerant, and scalable. We demonstrate our method in surface codes [60] and color codes [61], providing practical schemes for preparing encoded k-uniform states with near-term quantum devices.

Building on the preparation of encoded k-uniform states, we propose a hybrid physical-logical approach to reduce the overhead of arbitrary-angle logical rotations while preserving error-protection benefits. Conventional methods such as code switching [62], distillation [63,64], and cultivation [65] enable universal quantum computation but require substantial qubit and gate resources. Meanwhile, experimental platforms have achieved single-qubit gate fidelities exceeding 99.9%,

---

[*] Contact author: smajidy@fas.harvard.edu

©2025 American Physical Society

with some nearing 99.999% [66–68], suggesting that direct physical operations may be advantageous in certain regimes. To exploit this, we introduce a hybrid scheme that selectively unencodes qubits using hybrid physical-logical Bell states, applies physical arbitrary-angle rotations, and then reencodes them. Through exact numerical simulations with realistic noise models, we identify scenarios where the benefits of unencoding outweigh its costs for state preparation. Our results show that this hybrid approach can yield higher-fidelity physical state preparation than purely physical circuits, as demonstrated in k-uniform state preparation.

The remainder of this paper is organized as follows. In Sec. II we present our methods for (a) determining k uniformity of stabilizer states and (b) constructing scalable fault-tolerant circuits for preparing encoded k-uniform states. Section III demonstrates the application of this approach to surface and color codes. In Sec. IV we explore how logical k-uniform states can enhance the fidelity of physical state preparation within our hybrid scheme. Section V summarizes our findings and discusses future research directions.

II. CIRCUIT CONSTRUCTION METHOD

This section outlines our approach for identifying fault-tolerant scalable circuits that prepare encoded k-uniform states. In Sec. II A we describe how to determine k uniformity using a state's stabilizer tableau. Section II B then presents a circuit architecture designed for fault tolerance and scalability. This section provides an overview of our methodology, illustrative examples are provided in Sec. III, and a more technical and detailed summary is available in Appendix A. We denote a quantum code with n physical qubits, κ logical qubits, and distance d by $[[n, \kappa, d]]$, using κ instead of k to avoid confusion with k uniformity. Additionally, we denote the total number of qubits in the state by N.

A. Calculating *k* uniformity

Consider a stabilizer codespace for k qubits, defined by r stabilizer generators, which determines a set of 2^{k-r} codewords $|s_i\rangle$. The associated stabilizer mixed state is

$$\rho = \frac{1}{2^{k-r}} \sum_i |s_i\rangle\langle s_i|. \tag{1}$$

If $k = r$, ρ is a pure stabilizer state. More generally, for any N-qubit stabilizer state $|\psi\rangle$ and any subset A of qubits with $|A| = k$, one can always find a set of r stabilizer generators such that the reduced density matrix $\rho_A := \mathrm{Tr}_{\bar{A}}(|\psi\rangle\langle\psi|)$ is itself a stabilizer mixed state [69].

To assess approximate k uniformity, we employ the Δ-approximate criterion from Ref. [25]. A state $|\psi\rangle$ is Δ-approximate k uniform if

$$\|\mathrm{Tr}_{\bar{k}}(|\psi\rangle\langle\psi|) - I/2^k\|_1 \leqslant \Delta \tag{2}$$

for every size-k subset of qubits. Note that ρ_A and $I/2^k$ are diagonal in the codeword basis. The maximally mixed state has 2^k entries of 2^{-k}, while ρ_A has 2^{k-r} nonzero entries of $2^{-(k-r)}$. Thus, in the stabilizer-mixed case, this simplifies to $|\rho_A - I/2^k|_1 = 2 - 2^{1-r} \leqslant \Delta$, so determining Δ for $|\psi\rangle$ and k reduces to finding the maximum r over all subsets A with $|A| = k$.

We now describe how to extract this r from a stabilizer tableau. Let I_A be the number of stabilizer generators that remain independent when their action on $\bar{A}$ is replaced by the identity. From Ref. [70], the von Neumann entropy of the reduced density matrix satisfies

$$S(\rho_A) = I_A - k. \tag{3}$$

For stabilizer mixed states, ρ_A is diagonal in an appropriate basis, giving $S(\rho_A) = k - r$. Equating these expressions yields

$$r = 2k - I_A. \tag{4}$$

Thus, maximizing r is equivalent to minimizing I_A over all $|A| = k$ subsets. This provides a direct way to quantify a state's k uniformity from its stabilizer tableau.

For clarity, we now recast this result as a procedure for evaluating the k uniformity. Let $|\psi\rangle \in (\mathbb{C}^2)^{\otimes N}$ be a stabilizer state with stabilizer group $\mathcal{S} \subset \mathcal{P}_N$ of size $|\mathcal{S}| = 2^r$. Select r independent generators and represent them by a binary symplectic tableau $S \in \mathbb{F}_2^{2r\times N}$, where each row encodes the X and Z support of a Pauli operator. The procedure proceeds as follows.

(1) *Subsystem projection.* For each subset $A \subset [N]$ of size k, extract the $2r \times k$ submatrix S_A of S by retaining only the columns corresponding to the qubits in A.

(2) *Rank evaluation.* Compute the $\mathbb{F}_2$ rank of S_A, $I_A := \mathrm{rank}_{\mathbb{F}_2}(S_A)$, capturing the number of independent stabilizers supported on A.

(3) *Minimize over subsystems.* Repeat the above step for all $\binom{N}{k}$ such subsets and define $I_{\min} := \min_{|A|=k} I_A$.

(4) *Quantify deviation.* Set $r := 2k - I_{\min}$ and define the deviation from k uniformity as $\Delta := 2 - 2^{1-r}$. The state is exactly k uniform if $\Delta = 0$; otherwise, it is Δ-approximately k uniform in trace distance.

We illustrate the procedure using the logical $|\bar{0}\rangle$ state of the [[5,1,3]] code. The stabilizer group has $r = 5$ generators, represented by the binary symplectic tableau

$$S = \left[\begin{array}{ccccc|ccccc} 1 & 0 & 0 & 1 & 0 & 0 & 1 & 1 & 0 & 0 \\ 0 & 1 & 0 & 0 & 1 & 0 & 0 & 1 & 1 & 0 \\ 1 & 0 & 1 & 0 & 0 & 0 & 0 & 0 & 1 & 1 \\ 0 & 1 & 0 & 1 & 0 & 1 & 0 & 0 & 0 & 1 \\ 0 & 0 & 0 & 0 & 0 & 1 & 1 & 1 & 1 & 1 \end{array}\right]. \tag{5}$$

To test for $k = 2$ uniformity, we select the subset $A = \{2, 4\}$ and extract the corresponding submatrix

$$S_A = \left[\begin{array}{cc|cc} 0 & 1 & 1 & 0 \\ 1 & 0 & 0 & 1 \\ 0 & 0 & 0 & 1 \\ 1 & 1 & 0 & 0 \\ 0 & 0 & 1 & 1 \end{array}\right]. \tag{6}$$

The rank is $I_A = 4$. Exhaustive evaluation over all $\binom{5}{2} = 10$ subsets yields the same value. We compute the rank deficit as $r = 2k - I_A = 0$ and the corresponding deviation $\Delta = 2 - 2^{1-0} = 0$. We conclude that the five-qubit code state is exactly 2-uniform.

In certain settings, we are interested not in all k-qubit subsets, but only in those whose qubits are well separated

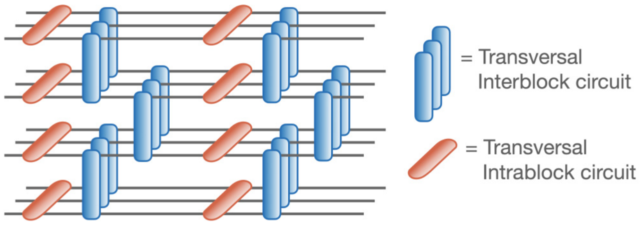
= Transversal Interblock circuit
= Transversal Intrablock circuit

FIG. 1. Fault-tolerant circuit architecture. For an $[[n, \kappa, d]]$ code, logical qubits are grouped into κ-qubit blocks. Transversal gates are applied within each block, followed by two-qubit transversal gates between neighboring blocks in a brickwork pattern.

in space. To formalize this, we introduce the notion of α-separated k uniformity: A state is α-separated k uniform if every subset of k qubits spaced by at least α positions exhibits k uniformity. For example, when $k = 4$ and $\alpha = 3$, one evaluates subsets such as $\{1, 4, 7, 10\}$.

We repeat the above procedure, but restrict attention to such well-separated subsets. We fix a linear ordering of the N qubits and define

$$\mathcal{A}_k^{(\alpha)} := \{A \subset [N] : |A| = k; |i - j| \geqslant \alpha \, \forall \, i, j \in A\}.$$

The diagnostic routine proceeds as before, applied to subsets $A \in \mathcal{A}_k^{(\alpha)}$.

B. Scalable and fault-tolerant architecture

We outline our method for constructing scalable fault-tolerant circuits that prepare encoded k-uniform states, beginning with a conceptual overview followed by a step-by-step procedure. A detailed technical description is provided in Appendix A.

1. Overview

A naive approach to generating k-uniform states is to randomly construct Clifford circuits and evaluate their k uniformity using the procedure outlined in Sec. II A. However, such circuits generally lack fault tolerance and scalability, require long-range interactions, and exhibit large circuit depths. To address these issues, we restrict our search to a structured class of Clifford circuits.

Figure 1 illustrates our design for an $[[n, \kappa = 3, d]]$ code. Logical qubits are grouped into blocks of size κ. The circuit first applies transversal gates within each block, followed by two-qubit transversal gates between adjacent blocks in a brickwork pattern. Because every gate is transversal, the circuit is inherently fault tolerant. Any product state that can be fault-tolerantly initialized serves as a suitable starting state, and we systematically search over circuits of this form.

To achieve scalability, we look for circuits with spatially invariant circuit layers and refine boundary gates as needed. This guarantees a consistent bulk structure, allowing us to verify k uniformity for large but finite N and confidently extend it to even larger N. We first check for α-separated k uniformity. Once we identify a circuit that meets this reduced condition, we verify full k uniformity by checking all remaining subsets, avoiding the need for an exhaustive Δ calculation at every step.

2. Procedure

The protocol proceeds in three stages.

(1) *Initialize code and target parameters.* Choose an $[[n, \kappa, d]]$ quantum error-correcting code and record its transversal gate set, which fixes the admissible layer operations. Set the targets (k, Δ) and choose a separable Clifford input state. Specify an upper bound $N_{\max}$ on the number of physical qubits, and initialize N as the smallest integer $>2k$ compatible with the code constraints.

(2) *Search for valid circuits at fixed N.* Set $\beta = 1$. Enumerate all depth-β Clifford circuits that can be constructed via alternating layers of transversal gates within each block, followed by two-qubit transversal gates between adjacent blocks in a brickwork pattern. For each circuit ζ simulate its output state and compute the α-separated k-uniformity deviation, denoted by $\Delta_\zeta^{(\alpha)}$. If $\Delta_\zeta^{(\alpha)} \leqslant \Delta$, include the circuit and resulting state in a candidate set $\tilde{\Theta}_N$.

Refine the candidate set by computing the unrestricted deviation Δ_ζ for each circuit in $\tilde{\Theta}_N$. Circuits satisfying $\Delta_\zeta \leqslant \Delta$ are added to the final set Θ_N.

If no valid circuits are found, increment the depth $\beta \leftarrow \beta + 1$ and repeat this stage.

(3) *Repeat for increasing system sizes.* If $N < N_{\max}$, increment the system size $N \leftarrow N + 1$. Reset the circuit index $\zeta = 0$ and return to the previous stage.

This procedure yields a family of Clifford circuits built from fault-tolerant gates native to the chosen code, each preparing a Δ-approximate k-uniform state. Repeating the search for increasing N can reveal scalable patterns, which can be identified by inspection. In particular, circuits with consistent bulk structure, up to boundary effects, can be generalized to larger sizes. The examples in the next section illustrate this.

III. EXAMPLE CIRCUITS

We illustrate our method with two representative quantum codes. First, we examine the rotated surface code, a widely implemented architecture in recent quantum error correction experiments [50–53]. Second, we consider the [[4,2,2]] two-dimensional (2D) color code, which exemplifies cases where $\kappa > 1$ and connects to multiple error-correcting code families, including hypercube quantum codes and hybrid classical-quantum codes [71–74]. We validate our approach for systems of up to 40 qubits. Since the circuit bulk follows a uniform structure with only minor boundary modifications, e.g., reversing a small number of controlled-not (CNOT) orientations, k uniformity is preserved as N increases.

A. Surface code

The rotated surface code has parameters $[[L^2, 1, L]]$ and the logical X, Z, and CNOT gates are transversal. Here L is a free parameter that adjusts the code distance at the cost of additional physical qubits. A transversal Hadamard gate H can be enacted by physically rotating the code block [50], but such midcircuit rotations are often impractical, so we omit midcircuit H gates. Figure 2 shows four circuits our search produced for $k = 1$–4, starting from the logical state $|0\rangle^{\otimes N}$.

A CNOT gate with the control qubit on top is referred to here as upward, while one with the control qubit on the bottom

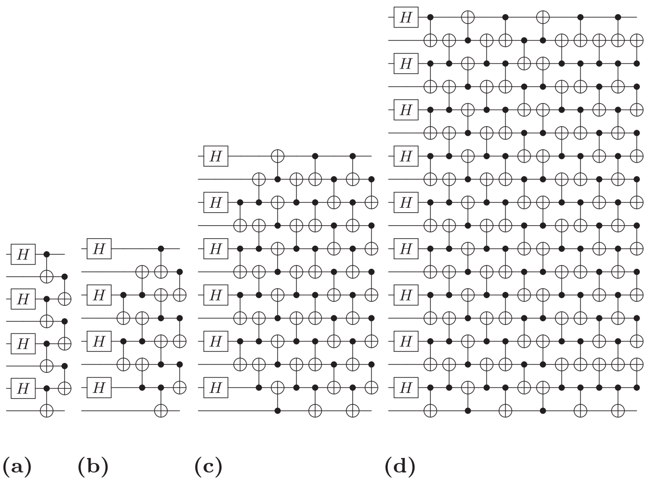

FIG. 2. State preparation circuits for the surface code for (a) $k=1$, (b) $k=2$, (c) $k=3$, and (d) $k=4$. In all cases, the initial state is $|0\rangle^{\otimes N}$. Our protocol imposes the following requirements: (a) $N \geqslant 2$, (b) $N \geqslant 6$, (c) $N \geqslant 12$, and (d) $N \geqslant 18$.

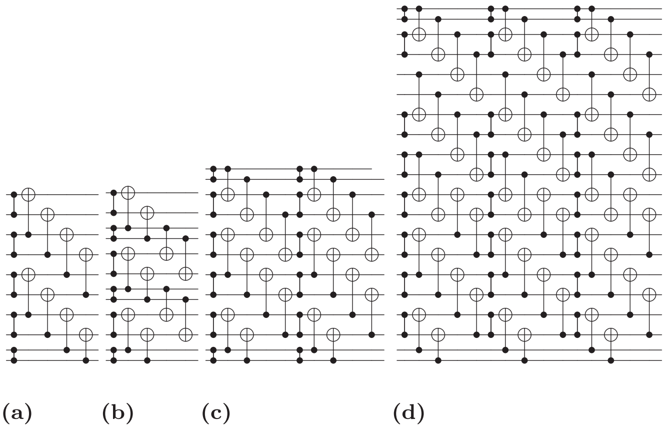

FIG. 3. State preparation circuits for the [[4,2,2]] color code for (a) $k=1$, (b) $k=2$, (c) $k=3$, and (d) $k=4$. In all cases, the initial state is $|+\rangle^{\otimes N}$. Our protocol imposes the following requirements: (a) $N \geqslant 2$, (b) $N \geqslant 6$, (c) $N \geqslant 10$, and (d) $N \geqslant 20$. For case (d), if $N/2$ is odd, the second-to-last cz gate is omitted instead of the last one.

is downward. For $k=1$, a single time step with two fully upward CNOT layers suffices. For $k=2$, the first and fourth CNOT layers are primarily upward, except for the outermost CNOT gates of the first layer which are removed, while the second and third layers are primarily downward, except for the outermost CNOT gates of the third layer which is downward. For $k=3$, the second to fourth layers are upward and the remaining layer are primarily upward, with the exception being the outermost CNOT gates of the first layer which are removed. For $k=4$, layers 2, 3, 4, 7, and 8 are downward, with other layers upward except for boundary gates in layers 10 and 12. In each case, the central portion of the circuit has a consistent structure, while only a few boundary gates are flipped to ensure full k uniformity for sufficiently large N.

B. Color code

To illustrate a code with $\kappa > 1$, we turn to the [4,2,2] 2D color code. This code supports transversal in-block X, Z, and cz gates, while interblock operations are realized via CNOT gates. We focus on circuits that begin in the product state $|+\rangle^{\otimes N}$. Higher connectivity allows for shorter circuit depths than in the surface code example. Exact k-uniform circuits for $k \leqslant 4$ appear in Fig. 3; they again share a uniform bulk structure with slight boundary gate modifications. For $k=1$, all cz gates appear within each block and all CNOT gates are oriented upward. For $k=2$, we start with the $k=1$ circuit and add a layer of downward-directed CNOT gates. For $k=3$, the circuit is constructed from two copies of the $k=1$ architecture, with the first four rows of CNOT gates reversed. For $k=4$, it is formed by combining three copies of the $k=1$ circuit, reversing the first ten rows of CNOT gates, omitting the third cz gate, and removing either the last or second-to-last cz gate, depending on the parity of $N/2$.

Beyond exact k-uniform states, Δ-approximate k-uniform states can be advantageous in applications such as product-formula simulations [25]. We set $\Delta = 1$ (the smallest nonzero value) to focus on larger k. In particular, for $k=5$, repeating one time step of the $k=3$ circuit three times suffices for $N \geqslant 20$. For $k=6$, five repetitions of one time step from the $k=1$ circuit work for $N \geqslant 24$. For $k=7$, five repetitions of the $k=3$ circuit suffice for $n \geqslant 32$. These smaller circuit depths reflect the relaxed requirement of Δ-approximate uniformity. Notably, increasing the depth of these circuits further does not continue to improve k uniformity (see Appendix C).

IV. HYBRID SCHEME AND PHYSICAL STATE PREPARATION

We now build on the circuits introduced in the preceding section to explore the hybrid scheme. We describe the hybrid scheme in Sec. IV A and present a more detailed exposition in Appendix B. A numerical comparison with a purely physical implementation follows in Sec. IV B. We do not compare against a fully logical, fault-tolerant scheme, as the hybrid approach is only relevant in resource-limited scenarios where such a scheme would be impractical. To maintain near-term feasibility, we focus on small-distance codes.

A. Hybrid scheme

We illustrate this scheme using a single logical qubit encoded in an $[[n, \kappa = 1, d]]$ code with logical operators $\bar{X}$ and $\bar{Z}$. The process begins by preparing a hybrid logical-physical Bell state

$$\frac{1}{\sqrt{2}}(|\bar{0}0\rangle + |\bar{1}1\rangle), \tag{7}$$

where the bar indicates that the qubit is logical.

There are multiple ways to generate this hybrid Bell state. One method constructs a circuit that prepares $|\bar{+}\rangle$ and couples it to a physical qubit via d CNOT gates, where the CNOT control qubits correspond to a representation of an X-type

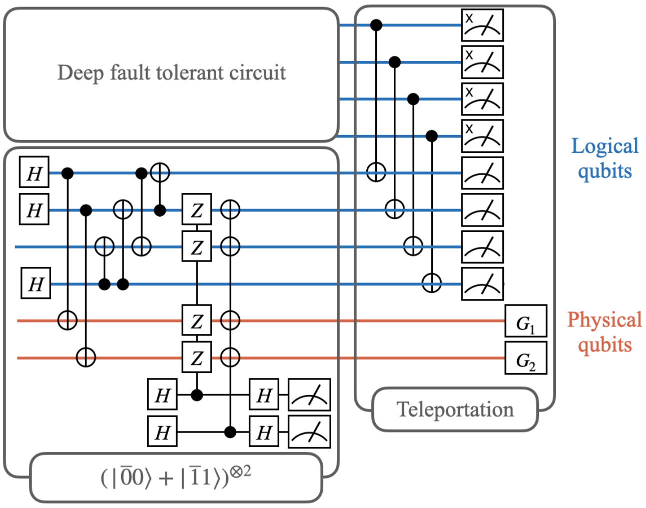
Deep fault tolerant circuit
Logical qubits
Physical qubits
H
Z
G_1
G_2
Teleportation
$(|\bar{0}0\rangle + |\bar{1}1\rangle)^{\otimes 2}$

FIG. 4. Example of the unencoding protocol for the [[4,2,2]] color code. The protocol begins with the preparation of the teleportation resource state $\frac{1}{\sqrt{2}}(|\bar{0}0\rangle + |\bar{1}1\rangle)$. Logical qubits are manipulated using their logical gate counterparts during the teleportation process. Correction gates G_1 and G_2 are applied based on measurement outcomes to complete the protocol.

logical operator and each target is the physical qubit. Circuit synthesis techniques can then minimize the number of operations on the physical qubit. Alternatively, one can prepare $|\bar{+}+\rangle$ and perform a $\bar{Z}Z$ measurement, postselecting on the desired outcome to obtain the target state. Another method first prepares a physical Bell state and then encodes one of its qubits, using, for instance, the technique described in Ref. [75].

After preparing the hybrid Bell state, we perform standard quantum teleportation. Specifically, we apply a CNOT gate between logical code blocks, measure all logical qubits in either the X or Z basis, and apply feedforward corrections on the physical qubit as needed. Figure 4 illustrates this process. Notably, this procedure can switch between any two codes, not just between a code and no code. Furthermore, since the only required gate is a fault-tolerant CNOT gate, our scheme applies to a broad class of codes, including all Calerbank-Shor-Steane (CSS) codes.

We present a few examples of circuits that prepare hybrid Bell states using the first method described. In each example, the final qubits represent the physical ones. For the [[7,1,3]] code [76], we simplified the circuit to require only a single gate on the physical qubit

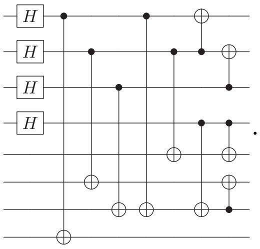

. (8)

For the [[9,1,3]] surface code, we also achieved a circuit with one CNOT gate on the physical qubit:

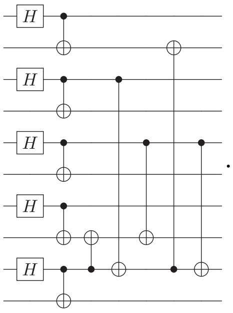

. (9)

For $\kappa > 1$, we need to create multiple pairs of Bell states. For instance, with the [[4,2,2]] code, we prepare

$$\frac{1}{4}(|\overline{00}00\rangle + |\overline{01}01\rangle + |\overline{10}10\rangle + |\overline{11}11\rangle) \tag{10}$$

by first creating $|\overline{++}\rangle$ and then coupling each physical qubit with d CNOT gates, followed by circuit simplification to achieve one CNOT gate per physical qubit:

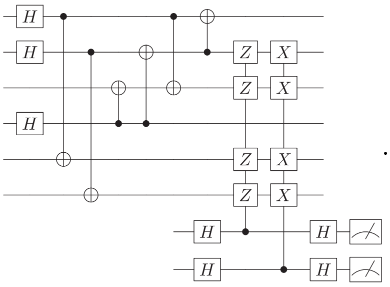

. (11)

New stabilizers can be introduced to track how errors propagate, which is presented in the above circuit. For example, an X error on the first qubit at the end of the circuit is detected after teleportation because it moves the logical state out of the code space, whereas an X error at the beginning may remain unnoticed by the teleportation measurements but still be flagged by an additional stabilizer.

B. Numerical comparison

The relative performance of the physical and hybrid schemes will naturally depend on the target state, its preparation method, and the choice of error-correcting code. To understand their relative advantages, we consider a few scenarios, beginning with one that favors the physical approach. We then examine more general cases, exploring quantum error detection and correction. Throughout this section, we model noise using one- and two-qubit depolarizing channels with error rates p_0 (idle), p_1 (single-qubit gates), p_2 (two-qubit gates), and p_3 (measurements).

To favor the physical approach we prepare a $k = 1$ uniform state using a minimum distance ($d = 2$) code. Furthermore, we study a $k = 1$ state whose circuits have been extensively optimized, the GHZ state. We consider two methods for preparing GHZ states. The first uses a constant-depth circuit with measurements and feedforward. For example, the

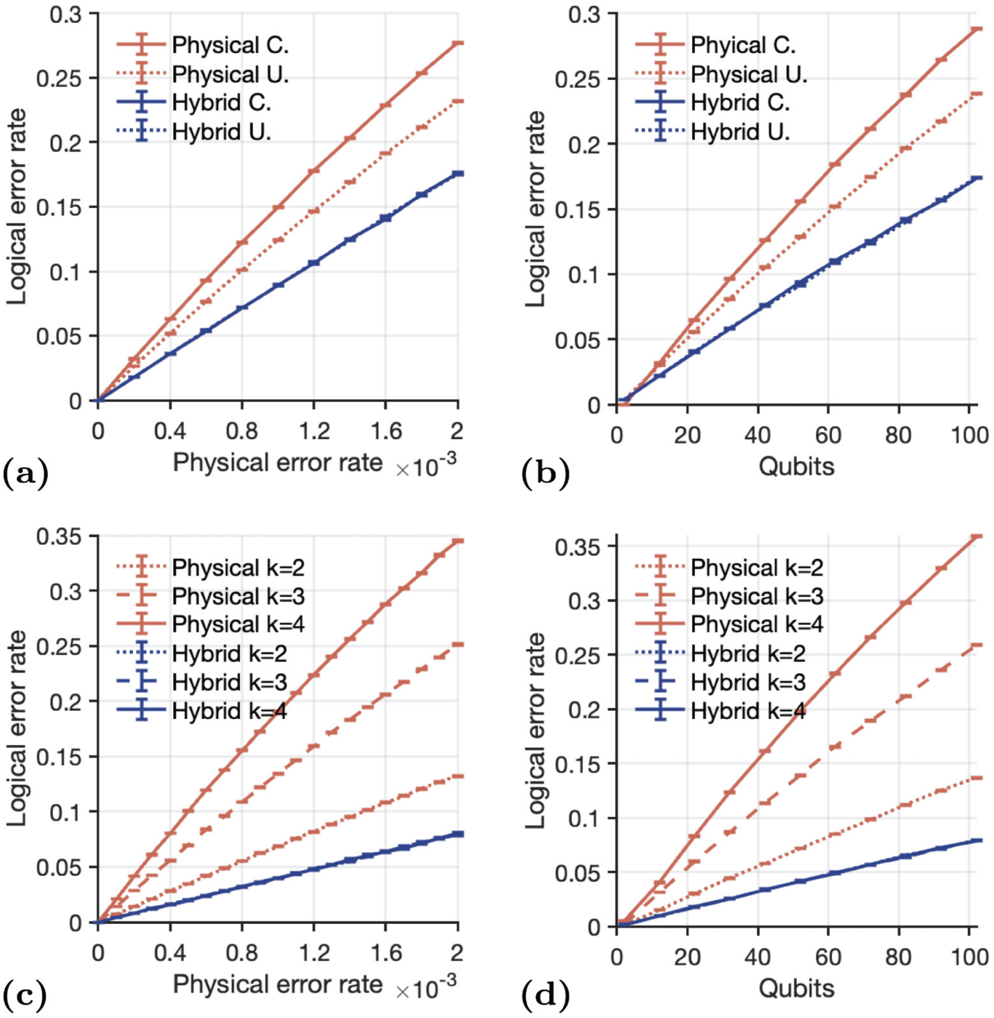

FIG. 5. Hybrid circuits outperforming physical circuits in state preparation even when using small distance codes: (a) and (b) GHZ preparation and (c) and (d) k-uniformm preparation. Shown is a numerical comparison of the hybrid and physical circuits in preparing physical k-uniform states under realistic noise models. For all plots we use 10^6 samples of the circuit. The error bars are included in all the figures but are too small to be clearly visible. For (a) and (c) we set the number of qubits equal to 50, $p_0 = p/100$, $p_1 = p/10$, and $p_2 = p_3 = p$; p is plotted on the x axis. For (b) and (d) we set $p_0 = 10^{-5}$, $p_1 = 10^{-4}$, $p_2 = 10^{-3}$, and $p_3 = 10^{-3}$. Here "C." and "U." stand for constant depth and unitary, respectively [see Eqs. (12) and (13)].

six-qubit GHZ state preparation circuit is

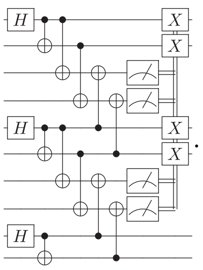

(12)

The second method avoids measurements and classical feed-forward corrections, but requires a deeper (logarithmic-depth) circuit. Below is an example circuit for an eight-qubit GHZ state:

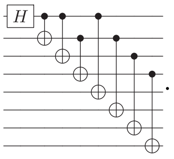

(13)

Figures 5(a) and 5(b) show the logical fidelity of these circuits as a function of qubit count and physical error rates for the hybrid and physical circuits. For the physical circuits, the constant-depth method results in lower fidelity than the logarithmic depth due to its higher number of physical gates per qubit. The hybrid circuits perform similarly, as both approaches are constrained by the same dominant error source: the non-fault-tolerant teleportation protocol. The hybrid scheme outperforms the physical one in both cases, with the advantage increasing as the error rate rises for a fixed qubit number and as the qubit number grows for a fixed error rate.

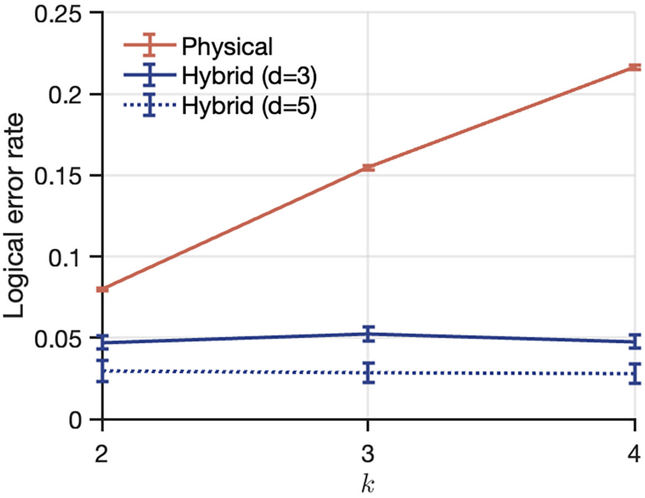

FIG. 6. Physical error rate increases with k, while hybrid error rate remains constant using the $[[L^2, 1, L]]$ surface code. Numerical comparison of the hybrid and physical circuit in preparing physical k-uniform states under realistic noise models. We set $p_0 = 10^{-5}$, $p_1 = 10^{-4}$, $p_2 = 10^{-3}$, $p_3 = 10^{-3}$, and the number of qubits equal to 30.

Next we extend our comparison to states with higher k, which require deeper circuits for physical preparation, as shown in Fig. 3. Figures 5(c) and 5(d) compare the resulting logical fidelity. In these cases, the hybrid method outperforms purely physical preparation. The key distinction lies in how error rates scale with increasing k. Physical circuits accumulate errors as depth increases, leading to progressively worse fidelity. Hybrid circuits maintain nearly constant error rates, since the limiting factor is the single non-fault-tolerant teleportation unencoding step. Once this step is performed, additional operations for increasing k uniformity do not introduce proportionally higher errors. This result highlights a fundamental advantage of hybrid approaches: They scale more robustly with circuit depth and complexity than purely physical implementations.

Finally, we highlight the improved scaling with k by analyzing k-uniform state preparation using the surface code circuits from Fig. 2 and incorporating quantum error correction. Figure 6 compares the hybrid scheme's performance for $d = 3$ and $d = 5$ surface codes. While the hybrid scheme maintains consistent performance with increasing k, purely physical preparation degrades with k.

V. DISCUSSION

Our work has demonstrated a scalable fault-tolerant method for preparing encoded k-uniform states. We introduced a stabilizer tableau-based technique to determine k uniformity and design fault-tolerant Clifford circuits for state preparation. Leveraging these states, we explored a hybrid physical-logical approach that balances some error protection with gate efficiency, showing its advantages over purely physical implementations for resource-state preparation. By extending k-uniform states into the logical space, our work paves the way for their use in key applications on physical quantum hardware.

Several promising directions emerge from this work. One avenue is to develop end-to-end protocols that utilize logical k-uniform states for specific applications, such as the various cryptographic applications [4–6]. Validating these protocols in real-world settings would not only confirm their theoretical benefits but also demonstrate their practical value. Another research direction involves exploring logical Δ-approximate k-uniform states, which can be prepared using shallower circuits than exact k-uniform states. Comparing their performance against exact states could offer valuable insights into their feasibility and usefulness on noisy quantum devices.

Finally, our hybrid scheme highlights additional opportunities for investigation. Here we focused on a single unencoding step, but an important question is whether iterating multiple rounds of encoding and unencoding can continue to provide an advantage. Identifying the scenarios in which such a repetitive approach is most beneficial, and whether it holds practical relevance remains an open challenge. In parallel, it is natural to compare this scheme against fully fault-tolerant methods or other $O(p)$ error techniques for implementing arbitrary angle rotations, in order to pinpoint which regimes each method best serves.

ACKNOWLEDGMENTS

We would like to thank Nishad Maskara and Madelyn Cain for many useful discussions. This work received support in part by the Banting Postdoctoral Fellowship and National Science Foundation QLCI Grant No. OMA-2120757. D.H. is grateful for support from the Simons Institute for the Theory of Computing, supported by U.S. DOE QSA.

DATA AVAILABILITY

The data that support the findings of this article are not publicly available upon publication because it is not technically feasible and/or the cost of preparing, depositing, and hosting the data would be prohibitive within the terms of this research project. The data are available from the authors upon reasonable request.

APPENDIX A: TECHNICAL SUMMARY OF METHOD

We provide a technical description of our methodology for identifying scalable fault-tolerant circuits that prepare logical k-uniform states. We adopt the notation from mathematics or computer science that $\leftarrow$ indicates a variable is being updated with a new value. Our method is as follows.

(1) Specify initial parameters.

(a) Select a quantum error-correcting code and list its transversal gates. The code's κ and gates determine the circuit architecture (see Fig. 1).

(b) Define the target k, Δ, and the initial state.

(c) Set the maximum qubit count $N_{\max}$ for the search. Start with N equal to the smallest integer strictly greater than $2k$ that fits the chosen architecture.

(2) Search for Δ-approximate k-uniform circuits. Estimate the minimal circuit depth β required to entangle k-qubit subsystems. This may be based on a light-cone argument or simply set to $\beta = 1$ to begin the search.

(a) Set the current sample index $\zeta = 0$.

(b) Identify a set of translationally invariant time steps.

(c) Enumerate all circuits of depth β consistent with step 1a, labeling them 0 to Z. Circuits with lower indices prioritize translationally invariant layers, with boundary modifications introduced progressively.

(d) For each circuit ζ, calculate α-separated Δ-approximate k uniformity. If Δ meets the target, include the circuit and state in $\tilde{\Theta}_n$.

(e) Increment ζ and repeat until all circuits are tested.

(f) Refine $\tilde{\Theta}_n$ by calculate the Δ-approximate k uniformity. If Δ equals the target Δ, include the circuit and state in the set Θ_n.

(g) If no circuits are found, increment $\beta \leftarrow \beta + 1$ and return to step 2

(3) Repeat for larger N. If $N < N_{\max}$, increment $N \leftarrow N + 1$ and return to step 2a.

At the end of this procedure, one has a set of circuits Θ_N for different values of N. To find a repeatable pattern, one can then identify a circuit architecture that remains consistent across all N. Next, verify that this architecture continues to prepare k-uniform states as N increases beyond $N_{\max}$, ensuring that the structure holds for all N with high confidence. Using this procedure, we obtain the circuits described in Sec. III.

APPENDIX B: HYBRID SCHEME SUMMARY

The hybrid scheme comprises two components: preparation of a hybrid Bell state and its use in quantum teleportation. We review each in turn.

1. Hybrid Bell state preparation

Let $\mathcal{C}$ be a CSS stabilizer code with parameters $[[n, \kappa, d]]$. We assume that the code admits a fault-tolerant procedure for preparing the logical state $|\bar{+}\rangle^{\otimes\kappa}$, where each logical qubit is in the $+1$ eigenstate of its logical $\bar{X}$ operator. Our goal is to prepare κ Bell pairs, i.e., an entangled state of the form

$$|\Phi_\kappa\rangle = \frac{1}{\sqrt{2}^{\kappa}}(|\bar{0}0\rangle + |\bar{1}1\rangle)^{\otimes\kappa}, \tag{B1}$$

where $|\bar{x}\rangle$ denotes the logical basis states of the code and $|x\rangle$ are the corresponding computational basis states of the physical qubits for $x \in \{0, 1\}$. This state acts as a resource for teleporting quantum information between encoded and unencoded registers. We now present two general methods for preparing $|\Phi_\kappa\rangle$.

Strategy 1: Joint stabilizer measurements.

(1) Start with the product state $|\bar{+}\rangle^{\otimes\kappa} \otimes |+\rangle^{\otimes\kappa}$.

(2) For each $i = 1, \ldots, \kappa$, define observables $Z_h^{(i)} = \bar{Z}_i \otimes Z_i$ and $X_h^{(i)} = \bar{X}_i \otimes X_i$.

(3) Measure each $Z_h^{(i)}$. If the outcome is -1, apply the correction $\bar{X}_i$ to the logical qubit. After this step, the joint state is in the $+1$ eigenspace of all $Z_h^{(i)}$.

(4) The resulting state is stabilized by all $X_h^{(i)}$ and $Z_h^{(i)}$ and is therefore equal to $|\Phi_\kappa\rangle$ in Eq. (B1).

This method requires κ joint measurements and κ conditional Pauli corrections. It works for any code where logical Pauli operators can be measured fault tolerantly and logical states $|\bar{+}\rangle^{\otimes\kappa}$ can be prepared fault tolerantly.

Strategy 2: Encoding half of a Bell state.

(1) Prepare a physical tensor product of κ physical Bell pairs

$$|\Phi_\kappa\rangle = \frac{1}{\sqrt{2}^{\kappa}}(|00\rangle + |11\rangle)^{\otimes\kappa}, \tag{B2}$$

where the first qubit in each of the κ pairs will serve as inputs to an encoder and the second qubit in each of the κ pairs will remain unencoded.

(2) Let U_{enc} denote an encoding circuit for the $[[n, \kappa, d]]$ stabilizer code $\mathcal{C}$, which maps computational basis states $|x\rangle$ to encoded basis states $|\bar{x}\rangle$, that is,

$$U_{\mathrm{enc}}(|x\rangle \otimes |0\rangle^{\otimes(n-\kappa)}) = |\bar{x}\rangle.$$

Note that such an arbitrary encoder is not fault tolerant.

(3) Apply U_{enc} to the first qubit in each of the κ pairs of $|\phi_\kappa\rangle$, together with $(n-\kappa)$ ancilla qubits initialized in $|0\rangle^{\otimes(n-\kappa)}$. This produces the state given in Eq. (B1).

This method avoids joint measurements and classical feedforward. However, it requires implementing a non-fault-tolerant encoding circuit U_{enc}. Which scheme is favorable will depend on the error model and gates available.

2. Hybrid teleportation

Once the entangled resource state in Eq. (B1) has been prepared, it can be used to teleport quantum information from κ logical qubits in one code block of the $\mathcal{C}$ into the κ physical qubits.

Let $|\bar{\Psi}\rangle = \sum_{x\in\{0,1\}^n} \alpha_x |\bar{x}\rangle$ denote the input logical state encoded in $\mathcal{C}$. We will call this the input code block. To teleport this state into the physical register of $|\Phi_\kappa\rangle$, we perform the following procedure.

(1) Since $\mathcal{C}$ is a CSS codes, it admits a transversal CNOT gate. Apply a transversal CNOT gate from the input logical block (control) to the logical half of the Bell pair (target).

(2) Measure each of the 2κ logical qubits across both blocks: Measure $\bar{X}_i$ on the input code block and measure $\bar{Z}_i$ on the resource code block. Let the outcomes of these 2κ Pauli measurements be recorded as classical bits: $s_i^{(X)} \in \{0, 1\}$ from measuring $\bar{X}_i$ and $s_i^{(Z)} \in \{0, 1\}$ from measuring $\bar{Z}_i$.

(3) For each $i = 1, \ldots, \kappa$, apply the Pauli correction $Z_i^{s_i^{(X)}} X_i^{s_i^{(Z)}}$ to the ith physical qubit. This completes the teleportation of the logical state $|\Psi\rangle_L$ into the physical register.

After this procedure, the κ physical qubits are in the state $\sum_{x\in\{0,1\}^n} \alpha_x |x\rangle$ and the two logical code blocks are disentangled and may be reset or discarded.

APPENDIX C: DECAY OF Δ-APPROXIMATE *k*-UNIFORM STATES

We can characterize Δ-approximate k-uniform states by their maximal deviation Δ and distribution across all k-site combinations. As n grows, the fraction of Δ-approximate

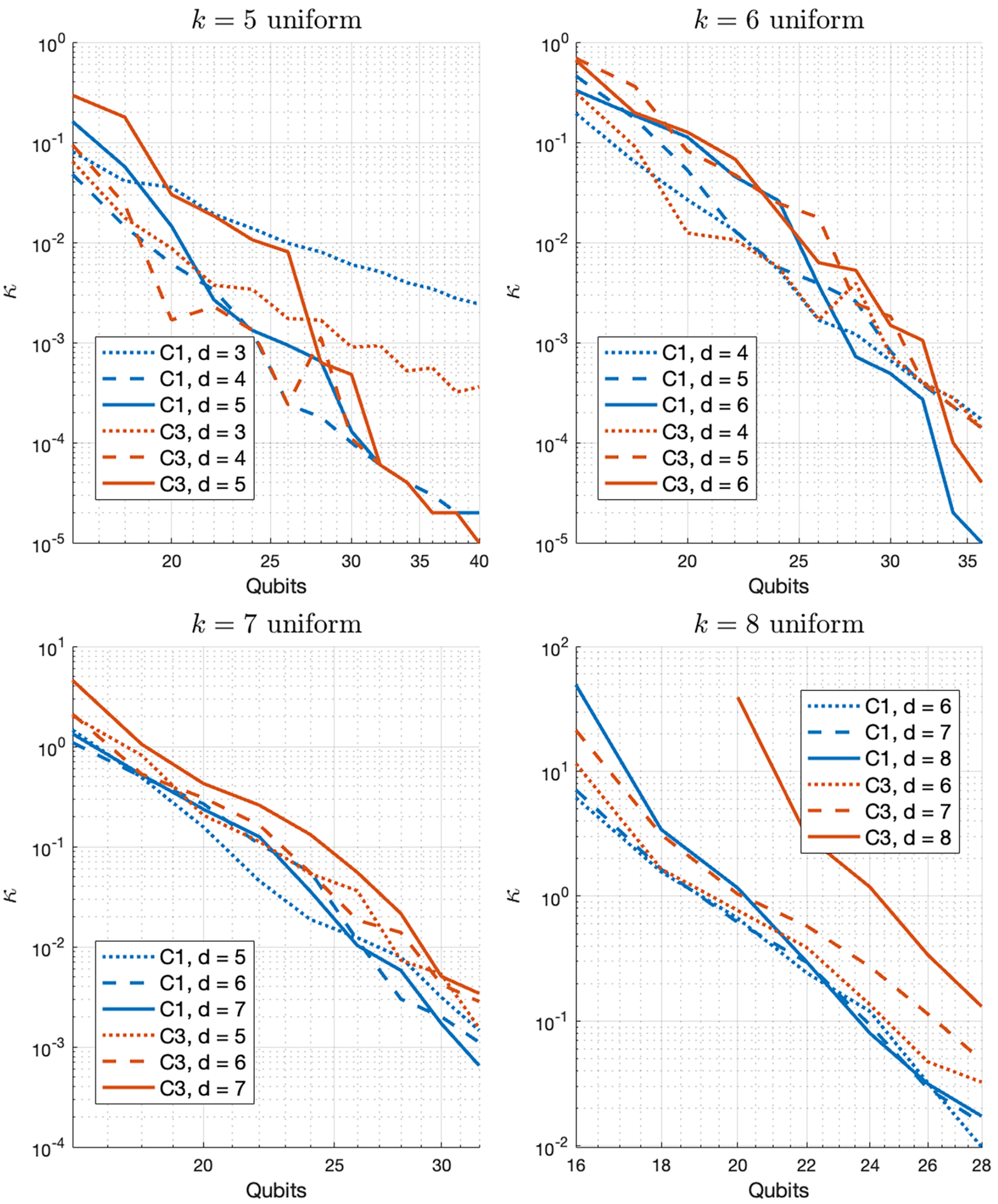

FIG. 7. Decay of non-k-uniform states for (a) $k = 5$, (b) $k = 6$, (c) $k = 7$, and (d) $k = 8$. Here κ denotes the ratio of Δ-approximate k-uniform subsets to those that are exactly k uniform. Circuits C_1 and C_3 correspond to layers identical to one time step of the circuits shown in Figs. 3(a) and 3(c), respectively. The circuit depth is denoted by d. The relative number of non-k-uniform states exhibits an approximate power-law decay with increasing circuit size.

k-uniform subsets relative to exact k-uniform ones decreases in an approximate power law (see Fig. 7). Notably, we see that simply adding more circuit layers does not prevent this decline.

---

[1] A. J. Scott, Multipartite entanglement, quantum-error-correcting codes, and entangling power of quantum evolutions, Phys. Rev. A **69**, 052330 (2004).

[2] P. Facchi, G. Florio, G. Parisi, and S. Pascazio, Maximally multipartite entangled states, Phys. Rev. A **77**, 060304(R) (2008).

[3] L. Arnaud and N. J. Cerf, Exploring pure quantum states with maximally mixed reductions, Phys. Rev. A **87**, 012319 (2013).

[4] W. Helwig, W. Cui, J. I. Latorre, A. Riera, and H.-K. Lo, Absolute maximal entanglement and quantum secret sharing, Phys. Rev. A **86**, 052335 (2012).

[5] W. Helwig and W. Cui, Absolutely maximally entangled states: Existence and applications, arXiv:1306.2536.

[6] F. Shi, M.-S. Li, L. Chen, and X. Zhang, k-uniform quantum information masking, Phys. Rev. A **104**, 032601 (2021).

[7] N. Paraskevopoulos, M. Steinberg, B. Undseth, X. Xue, A. Sarkar, L. M. Vandersypen, and S. Feld, Near-term spin-qubit architecture design via multipartite maximally-entangled states, PRX Quantum **6**, 020307 (2025).

[8] Z. Raissi, Modifying method of constructing quantum codes from highly entangled states, IEEE Access **8**, 222439 (2020).

[9] F. Pastawski, B. Yoshida, D. Harlow, and J. Preskill, Holographic quantum error-correcting codes: Toy models for the bulk/boundary correspondence, J. High Energy Phys. 06 (2015) 149.

[10] Z. Raissi, C. Gogolin, A. Riera, and A. Acín, Optimal quantum error correcting codes from absolutely maximally entangled states, J. Phys. A: Math. Theor. **51**, 075301 (2018).

[11] M. Steinberg, S. Feld, and A. Jahn, Holographic codes from hyperinvariant tensor networks, Nat. Commun. **14**, 7314 (2023).

[12] M. Steinberg, J. Fan, R. J. Harris, D. Elkouss, S. Feld, and A. Jahn, Far from perfect: Quantum error correction with (hyperinvariant) evenbly codes, Quantum **9**, 1826 (2025).

[13] C. Cao and B. Lackey, Approximate Bacon-Shor code and holography, J. High Energy Phys. 05 (2021) 127.

[14] F. Shi, K. Guo, X. Zhang, and Q. Zhao, Exploring quantum weight enumerators from the *n*-qubit parallelized swap test, arXiv:2406.18280.

[15] R. Laflamme, C. Miquel, J. P. Paz, and W. H. Zurek, Perfect quantum error correcting code, Phys. Rev. Lett. **77**, 198 (1996).

[16] E. Dennis, A. Kitaev, A. Landahl, and J. Preskill, Topological quantum memory, J. Math. Phys. **43**, 4452 (2002).

[17] T. Wagner, H. Kampermann, D. Bruß, and M. Kliesch, Pauli channels can be estimated from syndrome measurements in quantum error correction, Quantum **6**, 809 (2021).

[18] L. Borsten, D. Dahanayake, M. J. Duff, A. Marrani, and W. Rubens, Four-qubit entanglement classification from string theory, Phys. Rev. Lett. **105**, 100507 (2010).

[19] L. Borsten, M. Duff, A. Marrani, and W. Rubens, On the black-hole/qubit correspondence, Eur. Phys. J. Plus **126**, 37 (2011).

[20] J. K. Basak, V. Malvimat, and J. Yoon, A new genuine multipartite entanglement measure: From qubits to multiboundary wormholes, arXiv:2411.11961.

[21] D. Alsina and M. Razavi, Absolutely maximally entangled states, quantum-maximum-distance-separable codes, and quantum repeaters, Phys. Rev. A **103**, 022402 (2021).

[22] S. Popescu, A. J. Short, and A. Winter, Entanglement and the foundations of statistical mechanics, Nat. Phys. **2**, 754 (2006).

[23] M. Bilokur, S. Gopalakrishnan, and S. Majidy, Thermodynamic limitations on fault-tolerant quantum computing, arXiv:2411.12805.

[24] G. T. Landi, A. L. Fonseca de Oliveira, and E. Buksman, Thermodynamic analysis of quantum error-correcting engines, Phys. Rev. A **101**, 042106 (2020).

[25] Q. Zhao, Y. Zhou, and A. M. Childs, Entanglement accelerates quantum simulation, Nat. Phys. **21**, 1338 (2025).

[26] A. Borras, A. Plastino, J. Batle, C. Zander, M. Casas, and A. Plastino, Multiqubit systems: Highly entangled states and entanglement distribution, J. Phys. A: Math. Theor. **40**, 13407 (2007).

[27] Z. Raissi, A. Burchardt, and E. Barnes, General stabilizer approach for constructing highly entangled graph states, Phys. Rev. A **106**, 062424 (2022).

[28] S. Sudevan and S. Das, *n*-qubit states with maximum entanglement across all bipartitions: A graph state approach, arXiv:2201.05622.

[29] Z. Raissi, A. Teixidó, C. Gogolin, and A. Acín, Constructions of *k*-uniform and absolutely maximally entangled states beyond maximum distance codes, Phys. Rev. Res. **2**, 033411 (2020).

[30] K. Feng, L. Jin, C. Xing, and C. Yuan, Multipartite entangled states, symmetric matrices, and error-correcting codes, IEEE Trans. Inf. Theory **63**, 5618 (2017).

[31] W. Helwig, Absolutely maximally entangled qudit graph states, arXiv:1306.2879.

[32] M. Hein, J. Eisert, and H. J. Briegel, Multiparty entanglement in graph states, Phys. Rev. A **69**, 062311 (2004).

[33] F. Shi, Y. Shen, L. Chen, and X. Zhang, K-uniform states in heterogeneous systems, IEEE Trans. Inf. Theory **68**, 3115 (2022).

[34] Y. Zang, P. Facchi, and Z. Tian, Quantum combinatorial designs and k-uniform states, J. Phys. A: Math. Theor. **54**, 505204 (2021).

[35] M.-S. Li and Y.-L. Wang, *k*-uniform quantum states arising from orthogonal arrays, Phys. Rev. A **99**, 042332 (2019).

[36] S.-Q. Pang, X. Zhang, X. Lin, and Q.-J. Zhang, Two and three-uniform states from irredundant orthogonal arrays, npj Quantum Inf. **5**, 52 (2019).

[37] D. Goyeneche, Z. Raissi, S. Di Martino, and K. Życzkowski, Entanglement and quantum combinatorial designs, Phys. Rev. A **97**, 062326 (2018).

[38] D. Goyeneche, D. Alsina, J. I. Latorre, A. Riera, and K. Życzkowski, Absolutely maximally entangled states, combinatorial designs, and multiunitary matrices, Phys. Rev. A **92**, 032316 (2015).

[39] D. Goyeneche and K. Życzkowski, Genuinely multipartite entangled states and orthogonal arrays, Phys. Rev. A **90**, 022316 (2014).

[40] P. Facchi, G. Florio, U. Marzolino, G. Parisi, and S. Pascazio, Classical statistical mechanics approach to multipartite entanglement, J. Phys. A: Math. Theor. **43**, 225303 (2010).

[41] S. Di Martino, P. Facchi, and G. Florio, Feynman graphs and the large dimensional limit of multipartite entanglement, J. Math. Phys. **59**, 012201 (2018).

[42] Y. Ning, F. Shi, T. Luo, and X. Zhang, Linear programming bounds on *k*-uniform states, arXiv:2503.02222.

[43] F. Shi, Y. Ning, Q. Zhao, and X. Zhang, Bounds on *k*-uniform quantum states, IEEE Trans. Inf. Theory **71**, 413 (2025).

[44] F. Huber, O. Gühne, and J. Siewert, Absolutely maximally entangled states of seven qubits do not exist, Phys. Rev. Lett. **118**, 200502 (2017).

[45] F. Huber, C. Eltschka, J. Siewert, and O. Gühne, Bounds on absolutely maximally entangled states from shadow inequalities, and the quantum Macwilliams identity, J. Phys. A: Math. Theor. **51**, 175301 (2018).

[46] A. Burchardt and Z. Raissi, Stochastic local operations with classical communication of absolutely maximally entangled states, Phys. Rev. A **102**, 022413 (2020).

[47] W. Zhang, Y. Ning, F. Shi, and X. Zhang, Extremal maximal entanglement, Phys. Rev. A **111**, 052410 (2025).

[48] R. V and S. Aravinda, Multipartite entanglement measure: Genuine to absolutely maximally entangled, arXiv:2410.15864.

[49] D. Bluvstein, A. A. Geim, S. H. Li, S. J. Evered, J. Ataides, G. Baranes, A. Gu, T. Manovitz, M. Xu, M. Kalinowski *et al.*, Architectural mechanisms of a universal fault-tolerant quantum computer, arXiv:2506.20661.

[50] D. Bluvstein, S. J. Evered, A. A. Geim, S. H. Li, H. Zhou, T. Manovitz, S. Ebadi, M. Cain, M. Kalinowski, D. Hangleiter *et al.*, Logical quantum processor based on reconfigurable atom arrays, Nature (London) **626**, 58 (2024).

[51] R. Acharya, L. Aghababaie-Beni, I. Aleiner, T. I. Andersen, M. Ansmann, F. Arute, K. Arya, A. Asfaw, N. Astrakhantsev, J. Atalaya *et al.*, Quantum error correction below the surface code threshold, Nature (London) **638**, 920 (2025).

[52] G. Q. A. team, Suppressing quantum errors by scaling a surface code logical qubit, Nature (London) **614**, 676 (2023).

[53] S. Krinner, N. Lacroix, A. Remm, A. Di Paolo, E. Genois, C. Leroux, C. Hellings, S. Lazar, F. Swiadek, J. Herrmann *et al.*, Realizing repeated quantum error correction in a distance-three surface code, Nature (London) **605**, 669 (2022).

[54] B. W. Reichardt, A. Paetznick, D. Aasen, I. Basov, J. M. Bello-Rivas, P. Bonderson, R. Chao, W. van Dam, M. B. Hastings, A. Paz *et al.*, Logical computation demonstrated with a neutral atom quantum processor, arXiv:2411.11822.

[55] P. S. Rodriguez, J. M. Robinson, P. N. Jepsen, Z. He, C. Duckering, C. Zhao, K.-H. Wu, J. Campo, K. Bagnall, M. Kwon *et al.*, Experimental demonstration of logical magic state distillation, arXiv:2412.15165.

[56] M. Da Silva, C. Ryan-Anderson, J. Bello-Rivas, A. Chernoguzov, J. Dreiling, C. Foltz, J. Gaebler, T. Gatterman, D. Hayes, N. Hewitt *et al.*, Demonstration of logical qubits and repeated error correction with better-than-physical error rates, arXiv:2404.02280.

[57] Y. Hong, E. Durso-Sabina, D. Hayes, and A. Lucas, Entangling four logical qubits beyond break-even in a nonlocal code, Phys. Rev. Lett. **133**, 180601 (2024).

[58] C. Ryan-Anderson, N. Brown, C. Baldwin, J. Dreiling, C. Foltz, J. Gaebler, T. Gatterman, N. Hewitt, C. Holliman, C. Horst *et al.*, High-fidelity teleportation of a logical qubit using transversal gates and lattice surgery, Science **385**, 1327 (2024).

[59] S. Majidy, C. Wilson, and R. Laflamme, *Building Quantum Computers: A Practical Introduction* (Cambridge University Press, Cambridge, 2024).

[60] A. G. Fowler, M. Mariantoni, J. M. Martinis, and A. N. Cleland, Surface codes: Towards practical large-scale quantum computation, Phys. Rev. A **86**, 032324 (2012).

[61] M. Grassl, T. Beth, and T. Pellizzari, Codes for the quantum erasure channel, Phys. Rev. A **56**, 33 (1997).

[62] J. T. Anderson, G. Duclos-Cianci, and D. Poulin, Fault-tolerant conversion between the steane and Reed-Muller quantum codes, Phys. Rev. Lett. **113**, 080501 (2014).

[63] E. Knill, Fault-tolerant postselected quantum computation: Schemes, arXiv:quant-ph/0402171.

[64] S. Bravyi and A. Kitaev, Universal quantum computation with ideal Clifford gates and noisy ancillas, Phys. Rev. A **71**, 022316 (2005).

[65] C. Gidney, N. Shutty, and C. Jones, Magic state cultivation: Growing T states as cheap as CNOT gates, arXiv:2409.17595.

[66] D. A. Rower, L. Ding, H. Zhang, M. Hays, J. An, P. M. Harrington, I. T. Rosen, J. M. Gertler, T. M. Hazard, B. M. Niedzielski, M. E. Schwartz, S. Gustavsson, K. Serniak, J. A. Grover, and W. D. Oliver, Suppressing counter-rotating errors for fast single-qubit gates with fluxonium, PRX Quantum **5**, 040342 (2024).

[67] C. Löschnauer, J. M. Toba, A. Hughes, S. King, M. Weber, R. Srinivas, R. Matt, R. Nourshargh, D. Allcock, C. Ballance *et al.*, Scalable, high-fidelity all-electronic control of trapped-ion qubits, arXiv:2407.07694.

[68] S. J. Evered, D. Bluvstein, M. Kalinowski, S. Ebadi, T. Manovitz, H. Zhou, S. H. Li, A. A. Geim, T. T. Wang, N. Maskara *et al.*, High-fidelity parallel entangling gates on a neutral-atom quantum computer, Nature (London) **622**, 268 (2023).

[69] S. Aaronson and D. Gottesman, Improved simulation of stabilizer circuits, Phys. Rev. A **70**, 052328 (2004).

[70] A. Nahum, J. Ruhman, S. Vijay, and J. Haah, Quantum entanglement growth under random unitary dynamics, Phys. Rev. X **7**, 031016 (2017).

[71] B. Criger and B. Terhal, Noise thresholds for the [4, 2, 2]-concatenated toric code, Quantum Inf. Comput. **16**, 1261 (2016).

[72] A. Kubica, B. Yoshida, and F. Pastawski, Unfolding the color code, New J. Phys. **17**, 083026 (2015).

[73] S. Majidy, A unification of the coding theory and OAQEC perspectives on hybrid codes, Int. J. Theor. Phys. **62**, 177 (2023).

[74] J. M. Renes, F. Dupuis, and R. Renner, Efficient quantum polar coding, Phys. Rev. Lett. **109**, 050504 (2012).

[75] Y. Li, A magic state's fidelity can be superior to the operations that created it, New J. Phys. **17**, 023037 (2015).

[76] A. Steane, Multiple-particle interference and quantum error correction, Proc. R. Soc. London A **452**, 2551 (1996).